

Development of Free Cutting Steel without Lead Addition to Replace AISI12L14[†]

MURAKAMI Toshiyuki^{*1} TOMITA Kunikazu^{*2} SHIRAGA Tetsuo^{*3}

Abstract:

AISI12L14 (JIS SUM24L) is Pb-added free cutting steel containing 0.3% Pb and 0.3% S. Customers need Pb-free free cutting steel from the viewpoint of global environmental problems. Since it has long been known that the machinability of S-added free cutting steels is improved as the size of sulfide inclusions becomes larger, the improvement of machinability was studied from this viewpoint. Firstly, the chemical compositions of the developed steel were designed by the calculated phase diagram to have a wide temperature range of solidification which results in the formation of large size of sulfide inclusions. Based on the results, machinability test and hot forging test were actually conducted to confirm the chemical compositions. Crystallization of large sulfide inclusions was first attained with Cr addition and increment of S content. The authors have developed a new Pb-free free cutting steel with excellent machinability in a wide range from low cutting speed such as drilling to high one such as turning.

1. Introduction

Pb-added free cutting steel is widely used as a free cutting steel based on its ease of use. However, customers need Pb-free free cutting steel from the viewpoint of global environmental problems.

Free cutting steels can be broadly divided into two types. One type, represented by AISI12L14 (AISI: American Iron and Steel Institute), is a low carbon resulfurized Pb-added free cutting steel, in which good machinability is the primary requirement. The other type is a free cutting steel for machine structural use, in which cold forgeability and high strength are required

simultaneously with machinability¹⁾.

This paper describes a Pb-free free cutting steel which was developed as a low carbon resulfurized Pb-free free cutting steel to replace AISI12L14.

2. Background of Development

AISI12L14 (JIS SUM24L (JIS: Japanese Industrial Standards)) is a Pb-added low carbon resulfurized free cutting steel containing 0.3% Pb and 0.3% S. It is used in large quantities in automotive applications such as transmission oil hydraulic control valves and oil hydraulic hose connectors, and in printer shafts and other parts for office automation equipment. Because this free cutting steel has a remarkably high oxygen content on the order of 150 ppm, it was considered difficult to improve its machinability by adding Ca²⁾ or B³⁾ which is already used in the steel for machine structural use. Therefore, because it was necessary to consider other approaches, the authors focused on S, which is added in large quantity as an element which improves machinability. It has long been known that the machinability of S-added free cutting steel is improved as the size of sulfide inclusions becomes larger⁴⁾. From this viewpoint, the improvement of machinability by forming large sulfide inclusions was studied. Because the construction of thermodynamic databases for sulfides has advanced rapidly accompanying a progress in microalloying technology, this was effectively utilized in this study.

For developing the new steel, first, a phase diagram was obtained by the phase equilibrium calculation of a multi-component alloy system, and the alloy composition which could be expected to produce large sulfide inclusions was predicted. Based on the results, confirma-

[†] Originally published in *JFE GIHO* No. 23 (Mar. 2009), p. 17–23



^{*1} Senior Researcher,
Research and Development Dept.,
Sendai-Works,
JFE Bar & Shapes



^{*2} Dr. Eng.,
General Manager, Research and Development Dept.,
Sendai-Works,
JFE Bar & Shapes



^{*3} Dr. Eng.,
Fellow.,
JFE Bar & Shapes

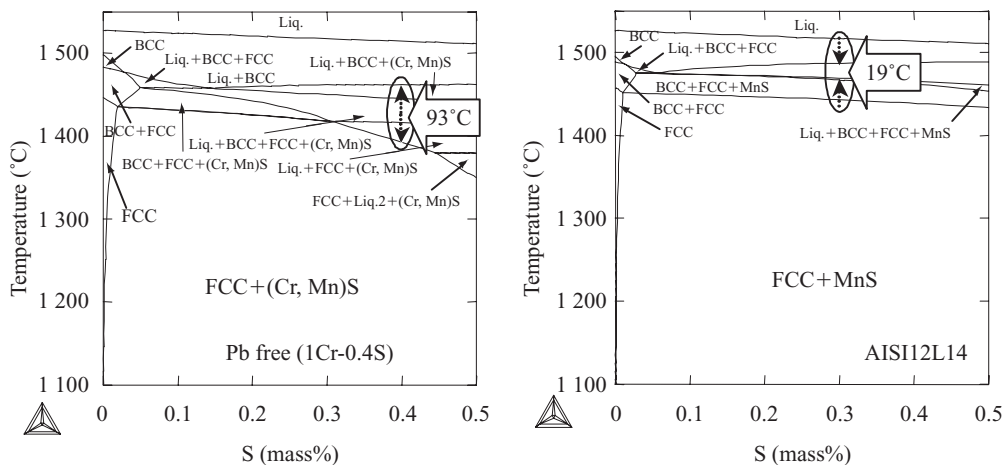


Fig. 1 Comparison of calculated phase diagram

tion tests were actually carried out, including melting, machinability tests, to decide the alloy composition. This new Pb-free free cutting steel was developed jointly with Prof. Kiyohito Ishida and Associate Prof. Katsunari Oikawa of Tohoku University.

3. Concept of Developed Steel

3.1 Prediction by Phase Diagram Calculation

The sulfide inclusions which contribute to machinability are crystallized by a monotectic reaction during the solidification of the molten steel. When attempting to obtain large inclusions, the following methods are conceivable.

- (1) Crystallization of large sulfide inclusions in the solidification stage
- (2) Reduction of the forging ratio after crystallization

In case of (1), the general practice is to retard the solidification rate, which can be achieved either by increasing the casting cross-sectional profile or by slow cooling during casting. However, in either case, it is difficult to effect large changes in the current continuous casting process. On the other hand, in case of (2), considering production of rolled material of the same size, a reduction in the forging ratio by using a smaller casting cross-sectional profile is conceivable, but as mentioned above, reducing the casting cross-sectional profile would result in a reduction in the size of the inclusions during casting, and thus would have little effect. Therefore, the authors considered a composition system which expands the temperature range in which sulfide inclusions crystallize from the liquid phase would be effective for securing large sulfide inclusions with the current continuous casting equipment.

In the study of the composition system, the authors focused on Cr for the following reasons:

- (1) Formation of (Cr, Mn)S and large sulfides can be expected.

- (2) (Cr, Mn)S also improves machinability.

- (3) Cr is not harmful to the environment as alloy element.

In the study to quantify the composition, phase diagrams were obtained by calculation and used to predict the crystallization temperature range for sulfide inclusions. In calculating these phase diagrams, a thermodynamic database for Fe-C-S-Cr-Mn system phase diagrams was constructed⁵⁾ using the CALPHAD (Calculation of Phase Diagrams) method, which is suitable for calculating the phase diagrams of multi-component alloy systems, and the phase diagram calculations were made using Thermo-Calc. (Thermo-Calc is a trade name and registered trademark of Thermo-Calc Software AB.) Although calculation was done for various compositions, it was found that no significant increase in the crystallization temperature range can be obtained by independently increasing S or adding only Cr; rather, the crystallization temperature range is only expanded by “Cr addition + S increment.” **Figure 1** shows an example of the calculated phase diagram of the developed steel in comparison with the calculated result for the conventional steel, AISI12L14.

With AISI12L14, the crystallization temperature range for sulfide inclusions is 19°C. In contrast, the temperature range of the developed steel expanded by more than four times, to 93°C. Next, the authors attempted to calculate the stage of solidification at which crystallization of sulfide inclusion begins with the composition system of the developed steel when the Cr content is changed. The calculated results are shown in **Fig. 2**. The stage of solidification at which crystallization of sulfide inclusions begins was calculated as a solid phase ratio of approximately 0.65, and this was substantially independent of the Cr content. Thus, it can be understood that crystallization of sulfide inclusions begins in the second half of solidification.

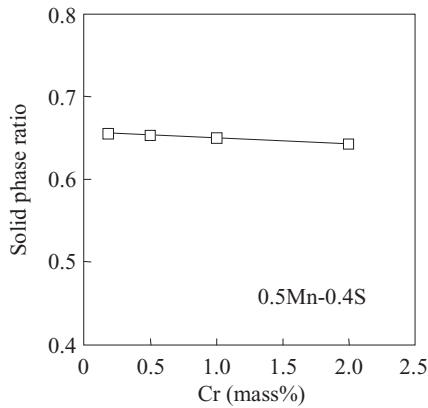


Fig. 2 Effect of Cr content on solid phase ratio

3.2 Confirmation Tests Using Experimental Melting Furnace Steel

Test melting and machinability test were actually carried out using the compositions under consideration as candidates for a new Pb-free free cutting steel among those studied by calculation, and the confirmation tests for the final alloy composition were performed.

The test samples were melted in a 150 kg vacuum melting furnace and cast into 160 mm square ingots. The ingots were heated to 1 200°C, and hot forging was performed to a diameter of 85 mm, followed by normalizing at 950°C. Machinability test was then performed. Hot ductility was also evaluated in order to study the composition with an increment of the S content.

First, the morphology of the sulfide inclusions was observed. **Photo 1** shows a comparison of the sulfide inclusions in the intermediate part of the L cross section of forged materials with a diameter of 85 mm. The temperatures shown in parentheses () indicate the crys-

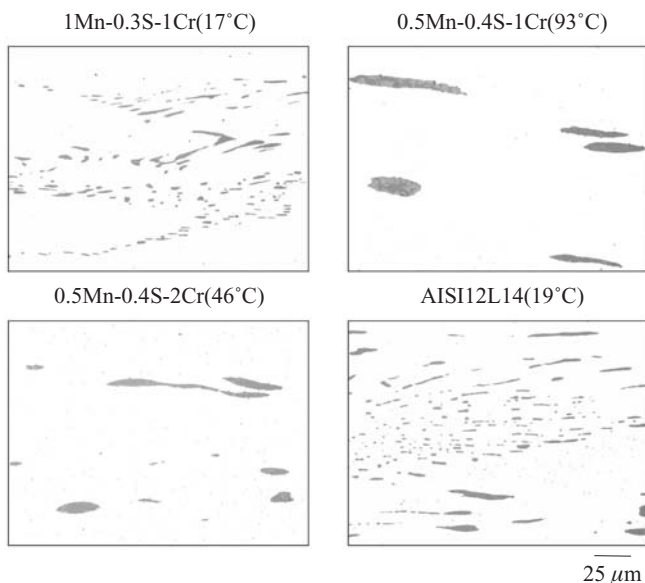


Photo 1 Comparison of size of sulfide inclusions ($\phi 85$)

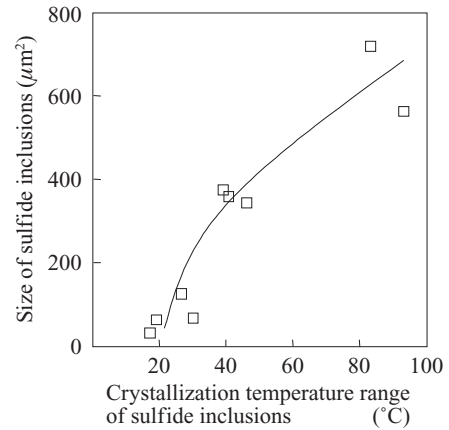


Fig. 3 Relationship between crystallization temperature range and size of sulfide inclusions

tallization temperature range of the sulfide inclusions obtained from the phase diagram calculations. The size of the sulfide inclusions in AISI12L14 was small. As in that steel, the size of the inclusions was also small in the 1Mn-0.3S-1Cr steel, which has the same composition as AISI12L14, but contains 1 mass% of added Cr. On the other hand, with the “Cr addition + S increment” systems, like those of 0.5Mn-0.4S-1Cr and 0.5Mn-0.4S-2Cr, large sulfide inclusions could be observed. **Figure 3** shows the relationship between the crystallization temperature range of the sulfide inclusions calculated in the phase diagram calculations for various composition systems and the size of the sulfide inclusions as measured from micrographs. The size of the sulfide inclusions was obtained by extracting the 5 largest sulfide inclusions from the micrographs and calculating their average area. The size of the sulfide inclusions increased as the crystallization temperature range expanded, which was consistent with predictions from the phase diagram calculations.

Next, machinability test was performed. Because good machined surface roughness is particularly required in parts using low carbon resulfurized (lead) free cutting steels, beginning with AISI12L14, which was the object of this study, first, a test of machined surface roughness was carried out. Machined surface roughness (maximum roughness) was measured after turning of 85 mm in diameter materials at various cutting speeds using a coated carbide tool, which is widely used by makers of machined parts. With all of the compositions, machined surface roughness decreased as the cutting speed increased. It was considered that the machined surface roughness decreased as the built-up edge on the tool surface became smaller and was eliminated. The relationship between the size of the sulfide inclusions and the machined surface roughness at a cutting speed of 100 m/min was arranged as shown in **Fig. 4**. Machined surface roughness decreased as the

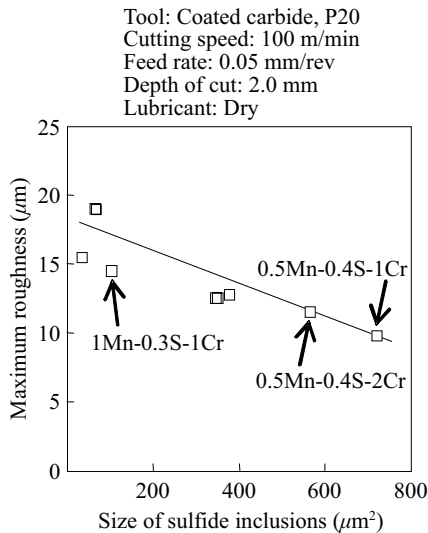


Fig. 4 Relationship between size of sulfide inclusions and maximum roughness

sulfide inclusions became larger in scale, confirming the effectiveness of large sulfide inclusions and the “Cr addition + S increment” composition in improving machined surface roughness. At the same time, a test of tool life and chip disposability was also performed. As in the case of machined surface roughness, the results confirmed that large sulfide inclusions and the “Cr addition + S increment” composition are also effective for improving these items.

In order to evaluate hot ductility, the condition of surface cracking of hot forged materials was observed. As evaluation items, in addition to opening of large surface cracks, surface cracking in which chipping of the turning tip or the high speed drill used in the machinability test was expected to occur during the test was also evaluated as a defect. The observed results were summarized in **Fig. 5**, which shows the effect of the Cr,

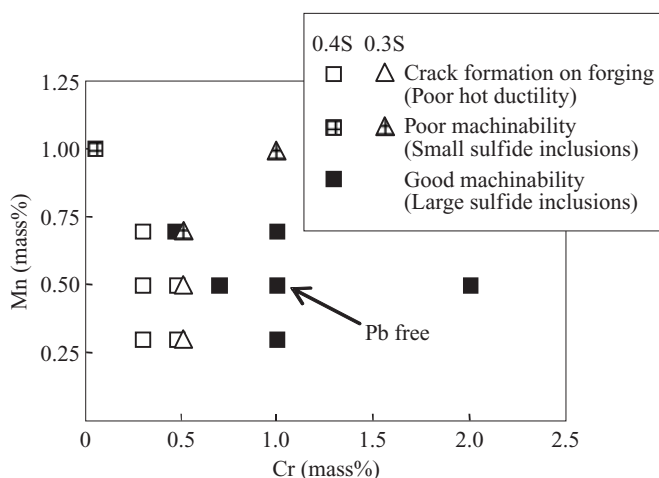


Fig. 5 Effect of Cr, Mn and S content in steel on machinability and hot ductility

Mn, and S contents on hot ductility, together with the results for machinability⁶⁾. Surface cracking occurred frequently in the low Cr, low Mn region, which is consistent with the hot ductility predicted from the solidus temperature. Furthermore, hot ductility improves as Cr is added or the Cr content is increased together with increasing the content of S, and at the same time, satisfactory machinability, as mentioned previously, is also secured by the large sulfide inclusions.

As described above, the 1mass%Cr-0.4mass%S steel was adopted as the new Pb-free free cutting steel which provides both satisfactory machinability and hot ductility, based on confirmation tests with experimental melting furnace steel conducted based on the predictions from the phase diagram calculations.

4. Properties of Developed Steel (Steel Melted in 130 t Electric Furnace)

4.1 Examples of Composition and Mechanical Properties

Table 1 shows an example of the chemical composition. **Table 2** shows mechanical properties. The mechanical properties of the developed steel are comparable to those of AISI12L14.

4.2 Comparison of Sulfide Inclusions

Photo 2 shows micrographs comparing the sulfide

Table 1 Chemical compositions

	(mass%)						
Steel	C	Si	Mn	P	S	Cr	Pb
Pb free	0.05	tr.	0.58	0.076	0.385	1.00	tr.
AISI12L14	0.07	tr.	1.05	0.070	0.340	0.08	0.24

Table 2 Mechanical properties (φ85)

Steel	YS (MPa)	TS (MPa)	El (%)	RA (%)
Pb free	298	401	36	57
AISI12L14	289	409	30	43

YS: Yield strength TS: Tensile strength
El: Elongation RA: Reduction of area

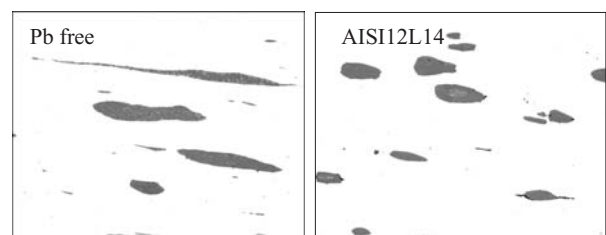


Photo 2 Comparison of size of sulfide inclusions (φ85)

Table 3 Partition of chromium

Steel	(mass%)					
	Ferrite			Sulfide		
	S	Mn	Cr	S	Mn	Cr
Pb free	0.026	0.15	0.94	36.9	41.7	10.2
AISI12L14	0.023	0.66	0.08	35.9	53.9	0.02

inclusions in the developed steel and AISI12L14. As examined thus far, the size of the sulfide inclusion of the developed steel is also larger in the steel melted in 130 t electric furnace. An element distribution of the sulfide inclusions in the developed steel using electron probe micro-analyzer (EPMA) detected S, Cr, and Mn in the inclusions as a whole. However, areas with high concentrations of Cr and areas with high concentrations of Mn were observed.

Cr was distributed in the sulfide inclusions, and was also distributed in the ferrite. Table 3 shows the results of a quantitative analysis of the ferrite and sulfide inclusions using EPMA. The partition ratio of Cr in the ferrite was high, reaching as much as approximately 0.9 mass%. It was considered that the dissolution of such high concentrations of Cr in the ferrite would affect strain ageing characteristics, and in turn, this would affect machinability, and particularly machined surface roughness. In order to study this effect, tests were performed with various Cr contents using a steel in which the main microstructure was ferrite with the same C content level of the developed steel and in which the S content was greatly reduced in order to eliminate the effect of sulfide inclusions. The results were confirmed that the effects of Cr on strain ageing characteristics and machined surface roughness were small⁷⁾. The same test was also performed using a steel which was added to the S content of 0.4 mass% such as the developed steel. In addition to considering the effect of strain ageing characteristics, the effects of sulfide inclusions were studied. In this case, the amount of sulfides increased as a result of S addition, and machined surface roughness became larger. However, when the size of the sulfide inclusions became larger as a result of simultaneously adding and increasing the content of Cr, machined surface roughness was reduced, accompanying combined addition of S and Cr. Thus, the results of these tests were also confirmed the effect of securing large sulfide inclusions by the “Cr addition + S increment” composition, which is the most important feature of the developed steel⁸⁾.

4.3 Machinability

Machinability was confirmed as being equal or superior to that of AISI12L14 under the conditions described below⁹⁾.

(1) Machinability in turning with carbide, coated carbide, and cermet tools (tool life and machined surface

roughness)

(2) Machinability in turning with high speed steel tool (tool life and machined surface roughness)

(3) Machinability in drilling with high speed steel tool (tool life)

(4) Chip disposability

Figure 6 shows the relationship between the number of holes and drill wear drilled with a 10 mm diameter high speed steel drill (JIS SKH51). With AISI12L14, drill wear progressed rapidly, abnormal sound could be heard during drilling after approximately 1 450 holes, and it became impossible to continue drilling. In contrast, no such phenomena were observed with the developed steel, and it was possible to drill more than 1 500 holes, showing satisfactory drilling machinability. Deburrability is also satisfactory, showing that the developed steel is also effective for improving burrs which must be treated manually.

Figure 7 shows the relationship between the cutting speed and machined surface roughness (maximum

Tool: SKH51 (ϕ 10) Hole depth: 30 mm
Feed rate: 0.35 mm/rev
Cutting speed: 63 m/min
Lubricant: Wet

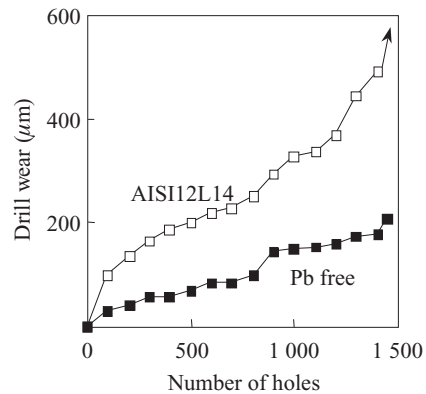


Fig. 6 Drill wear

Tool: Carbide, P20 Depth of cut: 2.0 mm
Lubricant: Dry

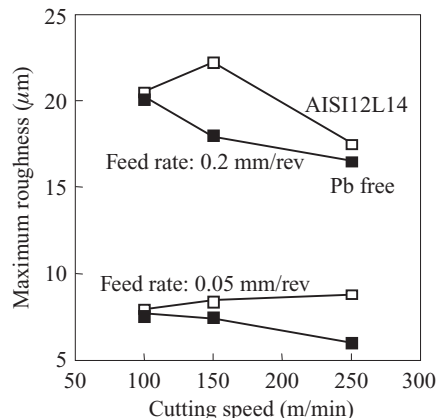


Fig. 7 Maximum roughness

roughness) in turning with a carbide tool (JIS P20). Although satisfactory machined surface roughness is particularly required in low carbon resulfurized (lead) free cutting steels, the machined surface roughness of the developed steel is satisfactory, being equal to or smaller than that of AISI12L14 at all cutting speeds.

Next, the mechanism responsible for imparting machinability in the developed steel will be described. The mechanisms of machinability in current free cutting steels can be broadly divided into the following four types. The effect of large sulfides, which is the most important feature of the developed steel, will be verified for each of these types.

(1) Easy Chip Formation by Notch Effect (S-Added Free Cutting Steel)

As shown previously in Photo 2, large sulfide inclusions are secured in the developed steel. Because larger sulfide inclusions are effective in preventing crack initiation and propagation, the developed steel is considered to have this effect.

(2) Embrittlement of the Material and Easy Chip Formation in the Shear Zone (S-Added Free Cutting Steel and Pb-Added Free Cutting Steel)

Pb-added free cutting steel has satisfactory chip disposability; however, this is because the melting point of the Pb which exists in the steel is low, which means that ductility decreases dramatically at around 300°C. In the warm working temperature range, which corresponds to this temperature, ductility decreases as the content of S in the steel increases. Because a rather large amount of S at 0.4 mass% is added to the developed steel, a decrease of ductility (i.e., embrittlement) is occurred in this temperature range. Therefore, the developed steel is considered to have this effect.

(3) Effect of Tool Face Lubrication (Lubrication Imparted at the Tool Face in Contact with the Chip or Work Piece; S-Added Free Cutting Steel and Pb-Added Free Cutting Steel)

This effect lowers the cutting resistance by imparting lubrication, which results from the existence of a sulfide film or molten Pb at the tool face in contact with the chip or work piece. Because a sulfide film of Cr-Mn-S was observed on the tool face after cutting in the analysis of the developed steel, the developed steel is considered to have this lubrication effect.

(4) Prevention of Diffusion Reaction between the Tool and Work Piece (Ca-Added Free Cutting Steel and BN-Added Free Cutting Steel)

It is widely known that a so-called belag with an oxide composition is formed and deposited on the tool face in cutting of Ca-added free cutting steel, and this is effective in suppressing tool wear. Tool wear is also suppressed by the formation and deposition

Table 4 Mechanism of developed free cutting steel

Effect	Drilling (Low speed)	Turning (High speed)
(1) Crack propagation	○	○
(2) Embrittlement of cutting zone	○	○
(3) Tool face lubrication	○	○
(4) Prevention of diffusion wear	×	×

○ : Effective × : Ineffective

of an AlN film in high speed cutting of BN-added free cutting steel, which is a Pb-free free cutting steel for machine structural use developed by JFE Bars & Shapes. In general, however, S-added free cutting steel does not have an effect of preventing the diffusion reaction between the tool and the work piece. Therefore, the developed steel, which is a type of S-added free cutting steel, is considered not to have this effect.

Table 4 summarizes the effects of the developed steel in imparting machinability, as described above, arranged by mechanism. The developed steel is effective for (1) to (3) in cutting from low speed drilling to high speed turning, but does not possess effect (4).

4.4 Carburization Characteristics

In some cases, low carbon resulfurized (lead) free cutting steel is used in parts which are carburized after cutting. Figure 8 shows the hardness distribution of the surface layer when gas carburizing was performed for 2 h at 930°C after machining of steels with a 10 mm square (length: 50 mm). The developed steel possesses carburization characteristics comparable to those of AISI12L14, showing virtually identical values for maximum hardness and effective case depth (threshold: 550HV0.3).

Figure 9 shows the results of a fatigue test after gas carburizing for 2 h at 870°C using an Ono-type rotating bending fatigue test piece. Both the fatigue limit and the

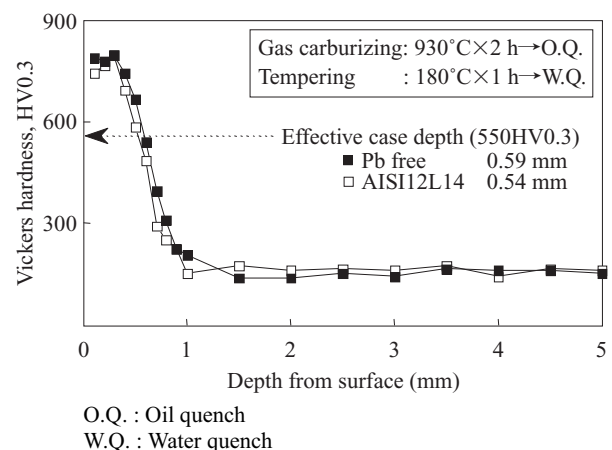


Fig. 8 Carburization characteristics

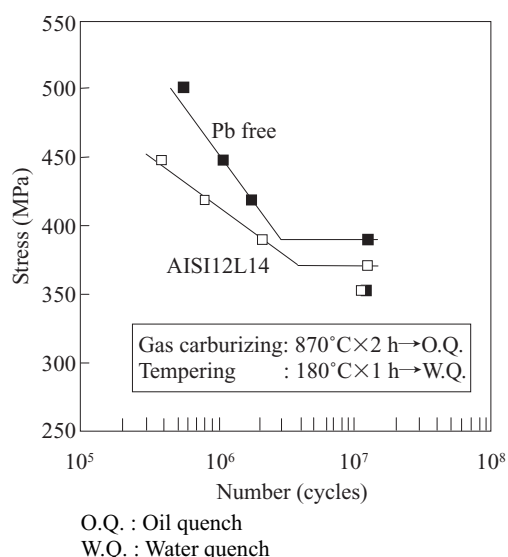


Fig.9 Fatigue characteristics

fatigue strength for finite life are higher with the developed steel than with AISI12L14, showing satisfactory fatigue characteristics.

4.5 Plating Characteristics

In some cases, machined parts are used in plated form, beginning with the printer shafts of office automation equipment. Therefore, the plating characteristics of the developed steel were evaluated by performing electroless Ni plating on drawn bars with a diameter of 10 mm. In order to confirm the effect of the surface condition before plating, specimens which had undergone a grinding process after drawing were tested. Plating characteristics were evaluated by measuring the plating film thickness, and the condition of occurrence of surface corrosion pits was measured by the rating number after a 2-h salt spray test. The results of these tests are shown in **Tables 5** and **6**, respectively. Regarding the plating film thickness, plating was performed using a control range of 3–6 μm as a plating condition. Both the developed steel and AISI12L14 were within this control range, and thus showed satisfactory film thicknesses. In the salt spray test, there was no difference in the rating numbers of the two steels, indicating that the developed steel possesses satisfactory corrosion resistance. The rating number of the grinded test piece was larger, and was satisfactory. Specimens were cut after plating in order to observe the condition of the plating layer/steel substrate interface. Concave parts were found on the steel substrate side in the non-grinded test piece, and initiation

Table 5 Comparison of plating film thickness

Steel	(μm)	
	Not grinded	Grinded
Pb free	4.017	4.548
AISI12L14	4.008	4.699

Table 6 Salt spray test result (Rating number)

Steel	Rating number	
	Not grinded	Grinded
Pb free	7	9
AISI12L14	7	9

of corrosion pits from these parts was confirmed. On the other hand, the plating layer/steel substrate interface of the grinded test pieces was smooth. This difference had affected corrosion pit initiation.

5. Conclusion

Pb-free free cutting steel to replace AISI12L14 was developed in response to customers' needs from the viewpoint of global environmental problems.

The developed steel features improved machinability by large sulfide inclusions. This was possible for the first time by adding Cr and further increasing the S content based on the estimation from the phase diagram calculations.

With the current tendency to reduce the use of Pb, expansion in the fields of application and quantity of this Pb-free free cutting steel is expected. Moreover, green procurement is also increasingly important in all industries, and the development of this new steel is expected to contribute to these efforts.

References

- 1) Murakami, T.; Tomita, K.; Shiraga, T. JFE Giho. 2009, no. 23, p. 10–16. (Japanese)
- 2) Ohno, T. 96th and 97th Nishiyama Memorial Seminar. ISIJ. Tokyo, 1984, p. 157–185. (Japanese)
- 3) Murakami, T.; Shiraga, T. NKK Technical Report. 2002, no. 178, p. 21–25. (Japanese)
- 4) Van Vlack, L. H. Trans. ASM. 1953, vol. 45, p. 741–746. (English)
- 5) Oikawa, K.; Mitsui, K.; Ishida, K. CAMP-ISIJ. 2003, vol. 16, p. 1516. (Japanese)
- 6) Murakami, T.; Shiraga, T.; Oikawa, K.; Ishida, K. CAMP-ISIJ. 2004, vol. 17, p. 1418. (Japanese)
- 7) Murakami, T.; Shiraga, T.; Oikawa, K.; Ishida, K. CAMP-ISIJ. 2006, vol. 19, p. 1011. (Japanese)
- 8) Murakami, T.; Shiraga, T. CAMP-ISIJ. 2007, vol. 20, p. 1004. (Japanese)
- 9) Murakami, T. The Special Steel. 2003, vol. 52, p. 22. (Japanese)